arXiv:hep-ph/9705401v1 23 May 1997

K-MATRIX ANALYSIS OF THE $K\pi$ S-WAVE IN THE MASS REGION $900-2100$ MEV AND NONET CLASSIFICATION OF SCALAR $q\bar{q}$-STATES

A.V. Anisovich and A.V. Sarantsev

Petersburg Nuclear Physics Institute
188350 Gatchina, Russia

Abstract

A K-matrix re-analysis of the $K\pi$ S-wave is performed in the mass region $900-2100$ MeV, and solutions which describe the data well are found. The solution with two resonances in the $(IJ^P = \frac{1}{2}0^+)$-wave has poles at (1415 ± 25)- $i(165 \pm 25)$ MeV and (1820 ± 40) -$i(125 \pm 50)$ MeV, close to the previous result of D. Aston et al., Nucl.Phys., B296 (1988) 493. The corresponding bare states, which are the subjects of a $q\bar{q}$ classification, are: $K_0^{bare}(1220^{+50}_{-60})$ and $K_0^{bare}(1885^{+50}_{-80})$. Within the restored bare states, a construction of the 1^3P_0 $q\bar{q}$ and 2^3P_0 $q\bar{q}$ nonets is completed. The three resonance solutions are analysed as well, the corresponding bare states are found, and the $q\bar{q}$-nonet classification is suggested. In all variants of our $q\bar{q}$-classification, the resonances $a_0(980)$ and $f_0(980)$ (or their bare counterparts) are non-exotic, and an extra scalar/isoscalar state exists in the mass region 1300-1700 MeV, being a good candidate for the lightest scalar glueball.

1 Introduction

The strategy for searching for exotic mesons, which is outlined in our recent investigations is based on a systematic classification of $q\bar{q}$ meson states: the extra states for such classification are to be considered as candidates for exotics (glueballs, hybrids, etc).

However, a systematization of the $q\bar{q}$ states at masses above 1000 MeV faces a serious problem: many of the observed resonances are products of the mixing caused by transitions $q\bar{q}$ *state* $\to$ *real mesons* $\to$ $q\bar{q}$ *state* at large distances, $r > R_{confinement}$. Correspondingly, the wave functions of the mixed states (resonances) contain the large-r multi-meson components with significant probabilities. The wave functions restored in such a way cannot be compared with the results of Strong-QCD models, which do not take into account the deconfinement of the quarks due to the resonance decay. For a comparision of the results of data-analysis with quark model calculations and for a classification of $q\bar{q}$-levels, one needs to separate large-r and small-r wave function components.

In refs. [1, 2], it was suggested to carry out the $q\bar{q}$ classification in terms of states which correspond to the K-matrix poles (bare states): their relation to the input poles of the propagator matrix (or D-matrix) is discussed in detail in ref.[3].

The K-matrix analysis of the (IJ^{PC}=00^{++})-wave which has been performed in the mass region 600-1950 MeV [2] points out an existence of five meson states: four of them should be considered as candidates for the members of two lightest nonets, $1^3P_0q\bar{q}$ and $2^3P_0q\bar{q}$, while the fifth state with the mass in the region 1250-1650 MeV is a good candidate for the scalar glueball. More detailed analysis of this wave carried out in terms of D-matrix and $q\bar{q}$ transition amplitudes [3, 4] confirms the results of ref.[2], restoring a quark/gluonium content of the observed resonances as well as the masses of non-mixed states (in particular, the mass of the pure scalar glueball which is the subject of the gluodynamic lattice calculations [5]).

Recently the K-matrix analysis was extended to the $IJ^{PC} = 10^{++}$ wave at 600-1800 MeV [6] thus allowing us to determine a_0^{bare}'s in this mass region. To a complete the construction of $1^3P_0q\bar{q}$ and $2^3P_0q\bar{q}$ nonets in terms of bare states, the K-matrix analysis of the $IJ^{PC} = \frac{1}{2}0^{++}$ state has to be performed: only after that one can definetely declare an exisance of extra states for the $q\bar{q}$ classification.

The classification of $\frac{1}{2}0^+$-resonances faces a problem: the mass of the lightest scalar K-meson, 1429 ± 9 MeV [7], is significantly higher then the masses the other lightest scalars, $f_0(980)$ and $a_0(980)$. In the set of papers (see, for example, [8]) the resonances $f_0(980)$ and $a_0(980)$ were considered as superfluous for the $q\bar{q}$ classification and the lightest scalar $q\bar{q}$ nonet was built from the higher resonances. Therefore, it is of key importance in a search for exotic mesons to perform the K-matrix analysis of the $\frac{1}{2}0^{++}$ wave. The present paper is devoted to this problem.

Let us stress that the identification of scalar/isoscalar resonances below 1950 MeV is quite reliable now because of significant progress during the few last years (see refs. [2, 9, 10] and references therein). The simultaneous analysis of Crystal Barrel [9], CERN-Münich [11], GAMS [12], and BNL [13] meson spectra performed in ref. [2] shows that the $IJ^{PC} = 00^{++}$ amplitude has five poles below 1900 MeV located at (in MeV units): $(1015 \pm 15) - i(43 \pm 8)$, $(1300 \pm 20) - i(120 \pm 20)$, $(1499 \pm 8) - i(65 \pm 10)$, $(1780 \pm 30) - i(125 \pm 70)$, $(1530^{+90}_{-250}) - i(560 \pm 140)$. The first four poles correspond to comparatively narrow resonances $f_0(980)$, $f_0(1300)$, $f_0(1500)$ and $f_0(1780)$; the fifth pole is related to a broad state defined in [2] as $f_0(1530^{+90}_{-250})$. The states $f_0(980)$ and $f_0(1500)$ are included now in the list of well defined resonances [14]. The properties of two states $f_0(1300)$ and $f_0(1530^{+90}_{-250})$ are collected together and defined as $f_0(1370)$ resonance in [14]. The resonance $f_0(1780)$ reproduces well the bump at 1750 MeV in $\pi\pi \to K\bar{K}$ data [13] and is partly responsible for the bump in the GAMS data on $\pi\pi \to \eta\eta'$ [12].

Correspondingly, the five bare states are unambiguously defined in [2]:

$$f_0^{bare}(720 \pm 100),\ f_0^{bare}(1235^{+150}_{-30}),\ f_0^{bare}(1260^{+100}_{-30}),\ f_0^{bare}(1600 \pm 50),\ f_0^{bare}(1810^{+30}_{-100}). \quad (1)$$

However, the $q\bar{q}$ classification of the bare scalar/isoscalar states faces uncertainties: there are two variants of the the construction of the $1^3P_0q\bar{q}$ and $2^3P_0q\bar{q}$ nonets related to a different choice of the bare state as the scalar gluonium. The source of such ambiguity is that the coupling constants for the gluonium decay coincide with that for transitions *$q\bar{q}$ bare state $\to$ two pseudoscalar mesons* at some definite $n\bar{n}/s\bar{s}$ content (here $n\bar{n} = (u\bar{u}+d\bar{d})/\sqrt{2}$): namely, at $\phi = 25^\circ - 30^\circ$ where ϕ is determined as $q\bar{q} = n\bar{n}\ \cos\phi + s\bar{s}\ \sin\phi$.

It results in two classification schemes [2]:

I. $f_0^{bare}(720)$ and $f_0^{bare}(1260)$ are members of the $1^3P_0 q\bar{q}$ nonet;
$f_0^{bare}(1600)$ and $f_0^{bare}(1810)$ are members of $2^3P_0 q\bar{q}$ nonet;
$f_0^{bare}(1235)$ is a glueball.

II. $f_0^{bare}(720)$ and $f_0^{bare}(1260)$ are members of the $1^3P_0 q\bar{q}$ nonet;
$f_0^{bare}(1235)$ and $f_0^{bare}(1810)$ are members of the first radial excitation nonet $2^3P_0 q\bar{q}$;
$f_0^{bare}(1600)$ is a glueball.

Such ambiguity in the classification is related to the close mixing angles and coupling constants for $f_0^{bare}(1230)$ and $f_0^{bare}(1600)$ states.

K-matrix analysis of isoscalar/tensor, isovector/scalar, and isovector/tensor amplitudes is performed recently in ref. [6]. The K-matrix approach, describing well the data, gives the following 10^{++} bare states:

$$a_0^{bare}(960 \pm 35),\ a_0^{bare}(1640 \pm 40)\ . \tag{2}$$

The partial wave analysis of the $K^-\pi^+$ system for the reaction $K^-p \to K^-\pi^+n$ at 11 GeV/c was performed by D.Aston et al. [7]. Two alternative solutions for the S-wave partial amplitude were obtained (following ref.[7] we call them solutions A and B); these solutions differ only at masses above 1800 MeV. In ref. [7], the analysis of the $K\pi$ S-wave was made separately for the mass regions $850 - 1600$ MeV and $1800 - 2100$ MeV, where the isospin 1/2 partial wave amplitude was parametrized as the sum of a Breit-Wigner resonance and a background term:

$$A_S^{1/2} = \sin\delta e^{i\delta} + \frac{M_R\Gamma_1}{(M_R^2 - M^2) - iM_R(\Gamma_1 + \Gamma_2)}\ . \tag{3}$$

Here Γ_1 and Γ_2 are partial widths for the resonance decay into $K\pi$ and $K\eta'$ channels. In the first mass region the resonance $K_0^*(1430)$ was found:

$$M_R = 1429 \pm 9\ \text{MeV}, \quad \Gamma = \Gamma_1 + \Gamma_2 = 287 \pm 31\ \text{MeV}\ . \tag{4}$$

In the second mass region, two solutions A and B give the following parameters for $K_0^*(1950)$:

$$\text{Solution A:} \qquad M_R = 1934 \pm 28\ \text{MeV}, \quad \Gamma = 174 \pm 98\ \text{MeV}. \tag{5}$$

$$\text{Solution B:} \qquad M_R = 1955 \pm 18\ \text{MeV}, \quad \Gamma = 228 \pm 56\ \text{MeV}. \tag{6}$$

However we believe that the analysis described above should be extended. First of all, the mass region $1600 - 1800$ MeV, where the amplitude varies rapidly, should not be excluded from the analysis. It is known from the analysis of the 00^{++} wave that, due to strong interference, the resonance can manifest itself not only as a peak in the spectrum but also as a dip or a shoulder: that happens for $f_0(980)$ and $f_0(1500)$ in the $\pi\pi$

scattering amplitude. Secondly, interference effects result in ambiguities. As a reminder, the ambiguities in 00^{++}-wave were resolved in [2] only due to a simultaneous fit of a number of different meson spectra; but there is no such variety of data for the $\frac{1}{2}0^+$ wave. So, one can expect that the solution found in [7] is not unique.

Concluding, the aim of the present investigation is:

(i) To restore the masses and the meson decay couplings of the scalar/isospin-$\frac{1}{2}$ bare states to perform a $q\bar{q}$-classification;

(ii) To obtain alternative K-matrix solutions for the $K\pi$ S-wave in the region below 2000 MeV.

2 K-matrix approach to the $K\pi$ S-wave amplitude.

The S-wave $K^-\pi^0$ scattering amplitude extracted from the $K^-p \to K^-\pi^+n$ reaction at small momentum transfer is a sum of the isospin-$\frac{1}{2}$ and isospin-$\frac{3}{2}$ components:

$$A_S = A_S^{1/2} + A_S^{3/2} =\mid A_S \mid e^{i\phi_S} \tag{7}$$

where $\mid A_S \mid$ and ϕ_S are measured magnitudes of the S-wave amplitude.

The isospin $I = 3/2$ component of the $K\pi$ S-wave amplitude is assumed to have non-resonant behaviour, so we use the following parameterization:

$$A_S^{3/2}(s) = \frac{\rho_1(s)a_{3/2}(s)}{1 - i\rho_1(s)a_{3/2}(s)}, \tag{8}$$

where $a_{3/2}(s)$ is written as

$$a_{3/2}(s) = a_{3/2} + \frac{f_{3/2}}{s - s_{3/2}}, \tag{9}$$

and $\rho_1(s)$ is the $K\pi$ phase volume:

$$\rho_1(s) = \sqrt{\left(1 - \frac{(m_K + m_\pi)^2}{s}\right)\left(1 - \frac{(m_K - m_\pi)^2}{s}\right)}\,. \tag{10}$$

For the description of the $A_S^{1/2}$ amplitude, we use the standard K-matrix representation:

$$A_S^{1/2} = K_{1a}\,(I - i\rho K)^{-1}_{a1} \tag{11}$$

where K_{ab} is a 3 x 3 matrix (a,b=1,2,3) with the following notations for meson channels:

$$1 = K\pi,\ 2 = K\eta',\ 3 = K\pi\pi\pi + multimeson\ states\,. \tag{12}$$

Including the resonance decay into the $K\eta$ channel does not affect the description of the data: the $K\eta$-coupling constant predicted by quark combinatoric rules is comparatively

small and agrees well with experimental data (see [7] and references therein). Thus, below we give the solutions where the $K\eta$-channel is omitted.

The phase space matrix is diagonal: $\rho_{ab} = \delta_{ab}\rho_a$ with ρ_1 defined by eq.(10) and ρ_2 is equal to:

$$\rho_2(s) = \sqrt{\Big(1 - \frac{(m_K + m_{\eta'})^2}{s}\Big)\Big(1 - \frac{(m_K - m_{\eta'})^2}{s}\Big)} \tag{13}$$

Below $K\eta'$ threshold, we use the analytic continuation of the phase space factor:
$\rho_2 = i \mid \rho_2 \mid$.

For the $K\pi\pi\pi + multimeson$ phase space factor at $s < 1.44$ GeV^2, we have used three alternative variants: it is defined either as

$$\rho_3(s) = C_1\Big(\frac{s - (m_K - 3m_\pi)^2}{s}\Big)^{5/2}, \quad s < 1.44 \text{ GeV}^2; \tag{14}$$

$$\rho_3(s) = 1, \quad s > 1.44 \text{ GeV}^2,$$

or as $\rho(770)K^*(892)$ and $\sigma K^*(892)$ phase space factors (σ stands for the low energy $\pi\pi$ S-wave amplitude):

$$\rho_3(s) = C_2 \int\limits_{(m_K+m_\pi)^2}^{(\sqrt{s}-2m_\pi)^2} dm_1^2 \int\limits_{4m_\pi^2}^{(\sqrt{s}-m_1)^2} dm_2^2 \frac{M_1 M_2 \Gamma_1 \Gamma_2}{((M_1^2 - m_1^2)^2 + M_1^2\Gamma_1^2)((M_2^2 - m_2^2)^2 + M_2^2\Gamma_2^2)}$$
$$\times\sqrt{\Big(1 - \frac{(m_1 + m_2)^2}{s}\Big)\Big(1 - \frac{(m_1 - m_2)^2}{s}\Big)}, \quad s < 1.44 \text{ GeV}^2; \tag{15}$$

$$\rho_3(s) = 1, \quad s > 1.44 \text{ GeV}^2.$$

Here M_a and Γ_a refer to the masses and widths of $K^*(892)$ and $\rho(770)$ (or $K^*(892)$ and σ). The factors C_i provide continuity of $\rho_3(s)$ at $s = 1.44$ GeV^2. The obtained characteristics of the $\frac{1}{2}0^+$-states do not depend significantly on the form used for $\rho_3(s)$: below we present results for $\rho_3(s)$ given by eq.(14).

For K_{ab}, we use the following parameterization:

$$K_{ab}(s) = \sum_\alpha \frac{g_a^\alpha g_b^\alpha}{M_\alpha^2 - s} \; + \; f_{ab}\frac{1.5 \text{ GeV}^2 - s_0}{s - s_0} \; . \tag{16}$$

The g_a^α are couplings of the bare states; the parameters f_{ab} and s_0 describe a smooth part (background) of K-matrix elements ($s_0 < 0$).

The $K^- p \to K^-\pi^+ n$ data were collected at small momenta transfer, ($|t| < 0.2$ GeV^2), so as a first step we have used to fit the data the unitary amplitude (11). As the next step, we have introduced a t-dependence into the K-matrix amplitude. For the amplitude $K\pi(t) \to K\pi$ (where $\pi(t)$ refers to a virtual pion) we write:

$$A_S^{1/2} = \tilde{K}_{1a}\,(I - i\rho K)^{-1}_{a1}, \tag{17}$$

where

$$\tilde{K}_{1a}(s) = \sum_{\alpha} \frac{g^{\alpha}(t) g_a^{\alpha}}{M_{\alpha}^2 - s} \; + \; f_a(t) \frac{1.5 \text{ GeV}^2 - s_0}{s - s_0}. \tag{18}$$

In the limit $t \to m_{\pi}^2$, the couplings $g^{\alpha}(t)$ and background terms $f_a(t)$ coincide with g_1^{α} and f_{1a} correspondingly. Taking into account that the momenta transfered are comparatively small, $|t| < 0.2$, we approximate $g^{\alpha}(t)$ and $f_a(t)$ as

$$g^{\alpha}(t) = u^{\alpha} g_1^{\alpha}, \qquad f_a(t) = u_a f_{1a} \tag{19}$$

where parameters u^{α} and u_a vary in the interval $0.9 - 1.1$.

In the leading terms of the $1/N$ expansion [15] , the couplings of the $q\bar{q}$-meson transition to two mesons are determined by the diagram shown in fig.1a where gluons produce a $q\bar{q}$-pair. The production of soft $q\bar{q}$ pairs by gluons violates flavour symmetry (see, for example, [2, 16, 17]): the quark production probability ratios are $u\bar{u} : d\bar{d} : s\bar{s} = 1 : 1 : \lambda$ with $\lambda = 0.45 - 0.8$. We fix in our fit $\lambda = 0.6$. This makes it possible to calculate the decay coupling constants in the framework of the quark combinatoric rules: they are given in Table 1 for both the leading terms of the $1/N$-expansion (process of the fig. 1a type) and for the next-to-leading terms (process of the fig 1b type). In the present fit, we have used the leading terms only.

3 Fit of the data and the $q\bar{q}$ classification schemes

In ref. [7] there are two solutions, A and B, for the $\frac{1}{2}0^+$ wave, which differ from each other at $M_{\pi K} > 1800$ MeV only. Correspondingly, we have got two K-matrix two-pole solutions, A-1 and B-1. In addition, for an analysis of alternatives, we have performed the K-matrix three-pole fits.

The solid curves in figs. 2-6 correspond to the description of the $K\pi$ wave defined by the unitary expression (11). The dashed curves show fits where t-dependence of the $K\pi$ interaction is taken into account by means of eq.(17). As it is seen, this dependence helps to describe phase shifts in the region 1700 MeV. Let us note that in this region (and in the region higher 2000 MeV in the solution A) the data violate unitarity limits. Such a strong violation is unlikely to be expected by t-dependence alone: we think it is connected with inaccurate PW analysis in this region performed in ref.[7]. However including t-dependence in our fits does not produce any serious effect either on masses of the bare states or on amplitude pole position. Usually, the masses of the bare states found in the t-dependant fits are at 20-30 MeV lower then those obtained in fits without t-dependence.

3.1 K-matrix two-pole solutions

The descriptions of the data for the data-sets A and B are shown in fig.2 (solutions A-1 and B-1). The K-matrix pole masses, coupling constants and pole position in the $K\pi \to K\pi$

S-wave scattering amplitude for both solutions are presented in Table 2. Both solutions give values of bare masses and amplitude pole positions which are rather close to each other. So we can treat these solutions as one:

$$K_0^{bare}(1220^{+50}_{-60})\,, \qquad K_0^{bare}(1885^{+50}_{-80})\,. \tag{20}$$

The $K\pi$ scattering amplitude in this case has the poles at

$$\begin{array}{rll} \text{II sheet} & M = 1415 \pm 25 - i\,(165 \pm 25) & \text{MeV} \\ \text{III sheet} & M = 1525 \pm 125 - i\,(420 \pm 80) & \text{MeV}. \\ \text{III sheet} & M = 1820 \pm 40 - i\,(125 \pm 50) & \text{MeV}. \end{array} \tag{21}$$

The definition of the sheets on the complex $M_{K\pi}$-plane is the following: II sheet is located under $K\pi$ and $K\pi\pi\pi$ cuts and the sheet III under $K\pi$, $K\pi\pi\pi$ and $K\eta'$ cuts. The state $K_0^{bare}(1220^{+50}_{-60})$ reveals itself as two poles of the amplitude in the region $M = 1400 - 1550$ MeV, where the $K\eta'$ threshold is located. This situation is analogous to that of $f_0(980)$: this is also realized as two poles near the $K\bar{K}$ threshold [18].

Classification of the bare scalar states based on eq. (20) is as follows:

$$1^3P_0: \quad f_0^{bare}(720 \pm 100),\ f_0^{bare}(1260^{+100}_{-30}),\ K_0^{bare}(1220^{+50}_{-60}),\ a_0^{bare}(960 \pm 30). \tag{22}$$

For the nonet of the first radial excitation, following [2], we have two cases. They are either Solution I:

$$\begin{array}{rl} 2^3P_0: & f_0^{bare}(1600 \pm 50),\ f_0^{bare}(1810^{+30}_{-100}),\ K_0^{bare}(1885^{+50}_{-80}),\ a_0^{bare}(1640 \pm 40), \\ \text{Glueball:} & f_0^{bare}(1235^{+150}_{-30}), \end{array} \tag{23}$$

or Solution II

$$\begin{array}{rl} 2^3P_0: & f_0^{bare}(1235^{+150}_{-30}),\ f_0^{bare}(1810^{+30}_{-100}),\ K_0^{bare}(1885^{+50}_{-80}),\ a_0^{bare}(1640 \pm 30) \\ \text{Glueball:} & f_0^{bare}(1600 \pm 50). \end{array} \tag{24}$$

Let us stress that the position of K-matrix poles in the $K\pi$-amplitude differ by about 100-200 MeV from the pole positions in scattering amplitudes; this is rather important from the point of view of the $q\bar{q}$ classification.

3.2 K-matrix three-pole solutions

We have performed two types of three-pole K-matrix fits. In one of them, the region $M_{\pi K} < 1600$ MeV is described by one pole, while for the region $M_{\pi K} > 1600$ MeV two K-matrix poles are used: these are Solutions A-2 and B-2.

For the next type of solution, we use two K-matrix poles for the region $M_{\pi K} < 1600$ MeV, while the region $M_{\pi K} > 1600$ MeV is described by one K-matrix pole, Solution B-3.

Solutions A-2 and B-2

Parameters of these solutions are given in Table 3. As before, the values of the K-matrix bare masses and positions of poles are close to each other for Solutions A-2 and B-2; thus

$$K_0^{bare}(1220 \pm 70)\,, \qquad K_0^{bare}(1860 \pm 90) \qquad K_0^{bare}(1975 \pm 115)\,. \tag{25}$$

The $K\pi$ scattering amplitude in this case has poles at

$$\begin{array}{rll} \text{II sheet} & M = 1420 \pm 30 - i\,(170 \pm 30) & \text{MeV} \\ \text{III sheet} & M = 1530 \pm 125 - i\,(400 \pm 150) & \text{MeV} \\ \text{III sheet} & M = 1815 \pm 40 - i\,(100 \pm 50) & \text{MeV.} \\ \text{III sheet} & M = 2010 \pm 90 - i\,(300 \pm 250) & \text{MeV.} \end{array} \tag{26}$$

Similarly to the previous solution, the state $K_0^{bare}(1220 \pm 70)$ reveals itself as two poles of the amplitude in the region $M = 1400 - 1550$ MeV, where the $K\eta'$ threshold is located.

Classification of the bare scalar states based on (25) is as follows:

$$1^3P_0: \quad f_0^{bare}(720 \pm 100),\ f_0^{bare}(1260^{+100}_{-30}),\ K_0^{bare}(1220 \pm 70),\ a_0^{bare}(960 \pm 30). \tag{27}$$

For the first radial excitation we have two cases again. Solution I:

$$\begin{array}{rl} 2^3P_0: & f_0^{bare}(1600 \pm 50),\ f_0^{bare}(1810^{+30}_{-100}),\ K_0^{bare}(1860 \pm 90),\ a_0^{bare}(1640 \pm 40), \\ \text{Glueball:} & f_0^{bare}(1235^{+150}_{-30}). \end{array} \tag{28}$$

Solution II:

$$\begin{array}{rl} 2^3P_0: & f_0^{bare}(1235^{+150}_{-30}),\ f_0^{bare}(1810^{+30}_{-100}),\ K_0^{bare}(1860 \pm 90),\ a_0^{bare}(1640 \pm 30) \\ \text{Glueball:} & f_0^{bare}(1600 \pm 50). \end{array} \tag{29}$$

Solution B-3

This solution differs from previous ones and gives quite different sets of states both for the 1^3P_0 nonet and for 2^3P_0. It has the following three bare K_0 states:

$$K_0^{bare}(1090 \pm 40)\,, \qquad K_0^{bare}(1375^{+125}_{-40}) \qquad K_0^{bare}(1950^{+70}_{-20})\,. \tag{30}$$

The $K\pi$ scattering amplitude in this case has poles at

$$\begin{array}{rll} \text{II sheet} & M = 998 \pm 15 - i\,(80 \pm 15) & \text{MeV} \\ \text{II sheet} & M = 1426 \pm 15 - i\,(182 \pm 15) & \text{MeV} \\ \text{III sheet} & M = 1468 \pm 30 - i\,(309 \pm 15) & \text{MeV} \\ \text{III sheet} & M = 1815 \pm 25 - i\,(130 \pm 25) & \text{MeV.} \end{array} \tag{31}$$

Classification of the bare scalar states based on eq.(30) is as follows:

$$1^3P_0: \quad f_0^{bare}(720 \pm 100),\ f_0^{bare}(1260^{+100}_{-30}),\ K_0^{bare}(1090 \pm 40),\ a_0^{bare}(960 \pm 30). \tag{32}$$

For the first radial excitation we have two cases again. Solution I:

$$\begin{aligned} 2^3P_0: &\quad f_0^{bare}(1600\pm 50),\ f_0^{bare}(1810^{+30}_{-100}),\ K_0^{bare}(1375^{+125}_{-40}),\ a_0^{bare}(1640\pm 40), \\ \text{Glueball:} &\quad f_0^{bare}(1235^{+150}_{-30}). \end{aligned} \tag{33}$$

Solution II:

$$\begin{aligned} 2^3P_0: &\quad f_0^{bare}(1235^{+150}_{-30}),\ f_0^{bare}(1810^{+30}_{-100}),\ K_0^{bare}(1375^{+125}_{-40}),\ a_0^{bare}(1640\pm 40) \\ \text{Glueball:} &\quad f_0^{bare}(1600\pm 50). \end{aligned} \tag{34}$$

In Solution B-3 the positions of bare states inside nonets are more compact.

4 Conclusion

We have performed the K-matrix analysis of the $\frac{1}{2}0^+$ wave, thus clarifying the situation with exotic mesons in the region of $900-1900$ MeV. Analysis shows that there is no basis to consider the resonances $f_0(980)$ and $a_0(980)$ as superfluous for $q\bar{q}$ classification: they are formed from the bare states which are members of the 1^3P_0 $q\bar{q}$ nonet. Two variants for this nonet are found which differ only in the mass of the lightest scalar kaon:

$$1^3P_0: \quad f_0^{bare}(720\pm 100),\ f_0^{bare}(1260^{+100}_{-30}),\ K_0^{bare}(1090\pm 40),\ a_0^{bare}(960\pm 30). \tag{35}$$

$$1^3P_0: \quad f_0^{bare}(720\pm 100),\ f_0^{bare}(1260^{+100}_{-30}),\ K_0^{bare}(1220\pm 70),\ a_0^{bare}(960\pm 30).$$

There are more possibilities in construction of the nonet 2^3P_0 $q\bar{q}$: they are given by eqs. (22), (23) and (33). But in all schemes, there exists one extra state, either $f_0^{bare}(1235)$ or $f_0^{bare}(1600)$, which should be classified as good candidates for the lightest scalar glueball. We remind that the state $f_0^{bare}(1600)$, as a candidate for the lightest glueball, is in agreement with the lattice gluodynamic calculations [5].

5 Acknowledgement

We thanks V.V.Anisovich and D.V.Bugg for usefull discussion and remarks.

This work was supported by RFFI grant 96-02-17934 and INTAS-RFBR grant 95-0267. A.V.A. is grateful for support from INTAS grant 93-0283-ext.

Table 1
Couplings $K_0 \to$ *two mesons* in the leading and next-to-leading terms of the $1/N$ expansion. Θ is the mixing angle for $\eta - \eta'$ mesons: $\eta = n\bar{n}\cos\Theta - s\bar{s}\sin\Theta$ and $\eta' = n\bar{n}\sin\Theta + s\bar{s}\cos\Theta$ where $n\bar{n} = (u\bar{u} + d\bar{d})/\sqrt{2}$.

Channel	Coupling constants in the leading $1/N_c$ terms	Next-to-leading terms
$K^-\pi^+$	$g^L/2$	0
$K^0\pi^0$	$g^L/\sqrt{8}$	0
$K^0\eta$	$(\cos\Theta/\sqrt{2} - \sqrt{\lambda}\sin\Theta)g^L/2$	$\left(\sqrt{2}\cos\Theta - \sqrt{\lambda}\sin\Theta\right) g^{NL}/2$
$K^0\eta'$	$(\sin\Theta/\sqrt{2} + \sqrt{\lambda}\cos\Theta)\ g^L/2$	$\left(\sqrt{2}\sin\Theta - \sqrt{\lambda}\cos\Theta\right) g^{NL}/2$

Table 2
The K-matrix parameters for solutions A-1 and B-1 and position of the poles in the scattering amplitude. A star denotes that the parameter is fixed. All values are given in GeV units.

Solution A-1		
$M_1 = 1.234 \pm 0.040$	$g_N^1 = 1.734^{+0.100}_{-0.200}$	$g_3^1 = 0.139 \pm 0.200$
$M_2 = 1.870^{+0.040}_{-0.070}$	$g_N^2 = 0.741 \pm 0.100$	$g_3^2 = 0.363 \pm 0.100$
$f_{11} = 0.832 \pm 0.20$	$f_{12} = 0.402 \pm 0.100$ $s_0 = -1.0^*$	$f_{13} = 0.250 \pm 0.100$
$a_{3/2} = 0. \pm 0.150$	$f_{3/2} = -1.200 \pm 0.200$	$s_{3/2} = 0^*$
II sheet poles		
1.427 ± 0.025 $-i\,(0.160 \pm 0.020)$		
III sheet poles		
1.525 ± 0.105 $-i\,(0.370 \pm 0.020)$	1.835 ± 0.030 $-i\,(0.106 \pm 0.020)$	
Solution B-1		
$M_1 = 1.202 \pm 0.045$	$g_N^1 = 1.812^{+0.100}_{-0.200}$	$g_3^1 = -0.048 \pm 0.150$
$M_2 = 1.900^{+0.040}_{-0.070}$	$g_N^2 = 1.035 \pm 0.100$	$g_3^2 = 0.414 \pm 0.100$
$f_{11} = 0.524 \pm 0.100$	$f_{12} = 0.226 \pm 0.100$ $s_0 = -1.0^*$	$f_{13} = -0.449 \pm 0.150$
$a_{3/2} = 0. \pm 0.150$	$f_{3/2} = -1.110 \pm 0.200$	$s_{3/2} = 0^*$
II sheet poles		
1.409 ± 0.015 $-i\,(0.185 \pm 0.015)$		
III sheet poles		
1.529 ± 0.125 $-i\,(0.545 \pm 0.050)$	1.806 ± 0.020 $-i\,(0.150 \pm 0.015)$	

Table 3
The K-matrix parameters for solutions A-2 and B-2 and position of the poles in the scattering amplitude. A star denotes that the parameter is fixed. All values are given in GeV units.

Solution A-2		
$M_1 = 1.235 \pm 0.040$	$g_N^1 = 1.739^{+0.100}_{-0.200}$	$g_3^1 = 0.112 \pm 0.100$
$M_2 = 1.810 \pm 0.040$	$g_N^2 = 0.454 \pm 0.100$	$g_3^2 = 0.391 \pm 0.100$
$M_3 = 1.947^{+0.070}_{-0.020}$	$g_N^3 = 0.493 \pm 0.150$	$g_3^3 = -0.368 \pm 0.100$
$f_{11} = 0.880 \pm 0.20$	$f_{12} = 0.430 \pm 0.100$ $s_0 = -1.0^*$	$f_{13} = 0.170 \pm 0.100$
$a_{3/2} = 0. \pm 0.150$	$f_{3/2} = -1.214 \pm 0.200$	$s_{3/2} = 0^*$
II sheet poles		
1.426 ± 0.030 $-i\ (0.157 \pm 0.025)$		
III sheet poles		
1.505 ± 0.035 $-i\ (0.360 \pm 0.015)$	1.795 ± 0.025 $-i\ (0.067 \pm 0.015)$	1.945 ± 0.025 $-i\ (0.068 \pm 0.015)$
Solution B-2		
$M_1 = 1.202 \pm 0.050$	$g_N^1 = 1.902^{+0.100}_{-0.200}$	$g_3^1 = 0.239 \pm 0.100$
$M_2 = 1.912 \pm 0.040$	$g_N^2 = 0.741 \pm 0.200$	$g_3^2 = 0.071 \pm 0.150$
$M_3 = 1.993 \pm 0.100$	$g_N^3 = 0.973 \pm 0.100$	$g_3^3 = 0.615 \pm 0.100$
$f_{11} = 0.648 \pm 0.100$	$f_{12} = 0.318 \pm 0.100$	$s_0 = -1.0^*$
$a_{3/2} = 0. \pm 0.150$	$f_{3/2} = -1.018 \pm 0.200$	$s_{3/2} = 0^*$
II sheet poles		
1.421 ± 0.015 $-i\ (0.186 \pm 0.015)$		
III sheet poles		
1.549 ± 0.105 $-i\ (0.430 \pm 0.125)$	1.836 ± 0.020 $-i\ (0.115 \pm 0.035)$	2.079 ± 0.030 $-i\ (0.475 \pm 0.315)$

Table 4
The K-matrix parameters for solution B-3. and position of the poles in the scattering amplitude. A star denotes that the parameter is fixed. All values are given in GeV units.

Solution B-3		
$M_1 = 1.090 \pm 0.040$	$g_N^1 = 1.545^{+0.200}_{-0.200}$	$g_3^1 = 1.195 \pm 0.100$
$M_2 = 1.375^{+0.125}_{-0.040}$	$g_N^2 = 0.685 \pm 0.600$	$g_3^2 = -1.085 \pm 0.600$
$M_3 = 1.950^{+0.070}_{-0.020}$	$g_N^3 = 1.239 \pm 0.100$	$g_3^3 = 0.601 \pm 0.600$
$f_{11} = 0.176 \pm 0.100$	$f_{12} = 0.093 \pm 0.100$ $s_0 = -1.0^*$	$f_{13} = -0.453 \pm 0.150$
$a_{3/2} = 0. \pm 0.150$	$f_{3/2} = -1.206 \pm 0.200$	$s_{3/2} = 0^*$
	II sheet poles	
0.998 ± 0.015 $-i\ (0.079 \pm 0.015)$	1.426 ± 0.015 $-i\ (0.182 \pm 0.015)$	
	III sheet poles	
	1.468 ± 0.050 $-i\ (0.309 \pm 0.015)$	1.815 ± 0.025 $-i\ (0.130 \pm 0.020)$

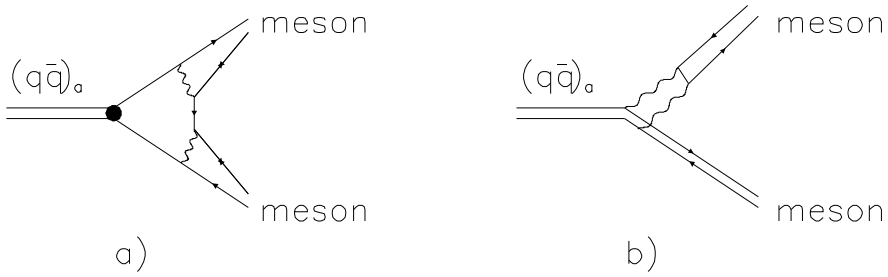

Fig. 1. Diagrams of $(q\bar{q})_a$-meson decay.

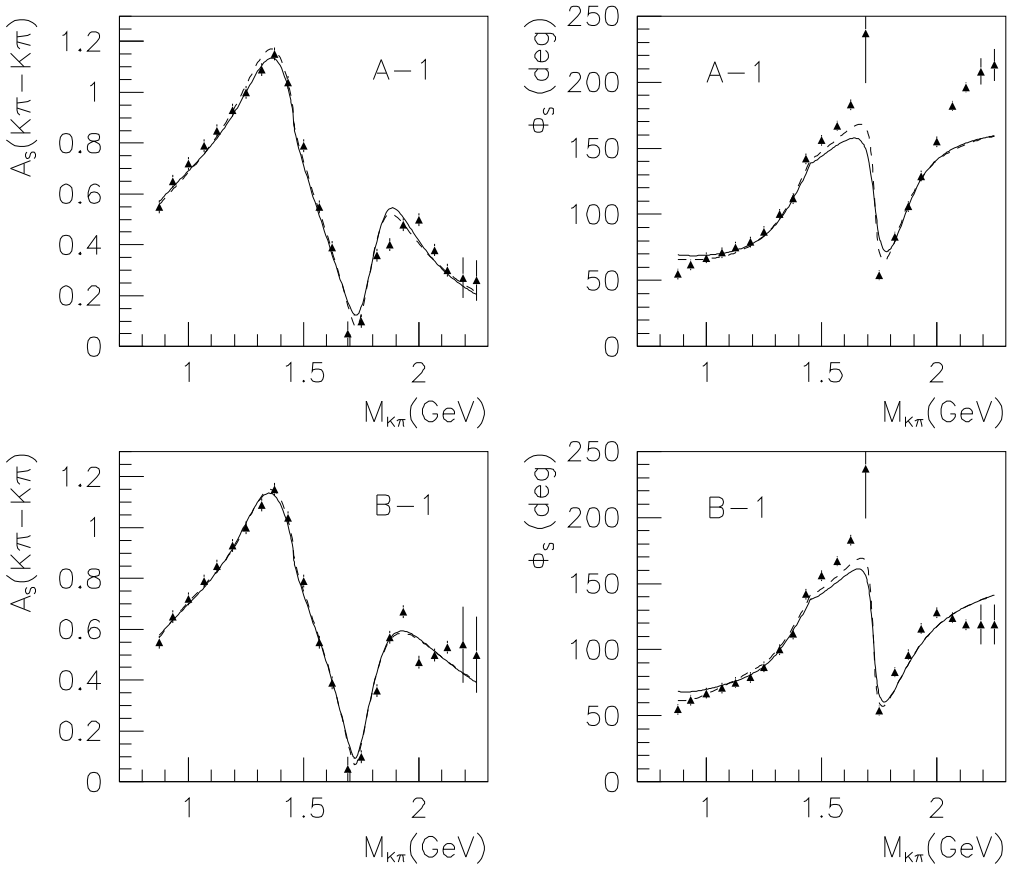

Fig. 2. The description of the data sets A and B from ref. [7] by the two-pole K-matrix solutions A-1 and B-1. The solid curves correspond to the fit with unitar expression for isospin 1/2 amplitude and the dashed ones to the t-dependant fit.

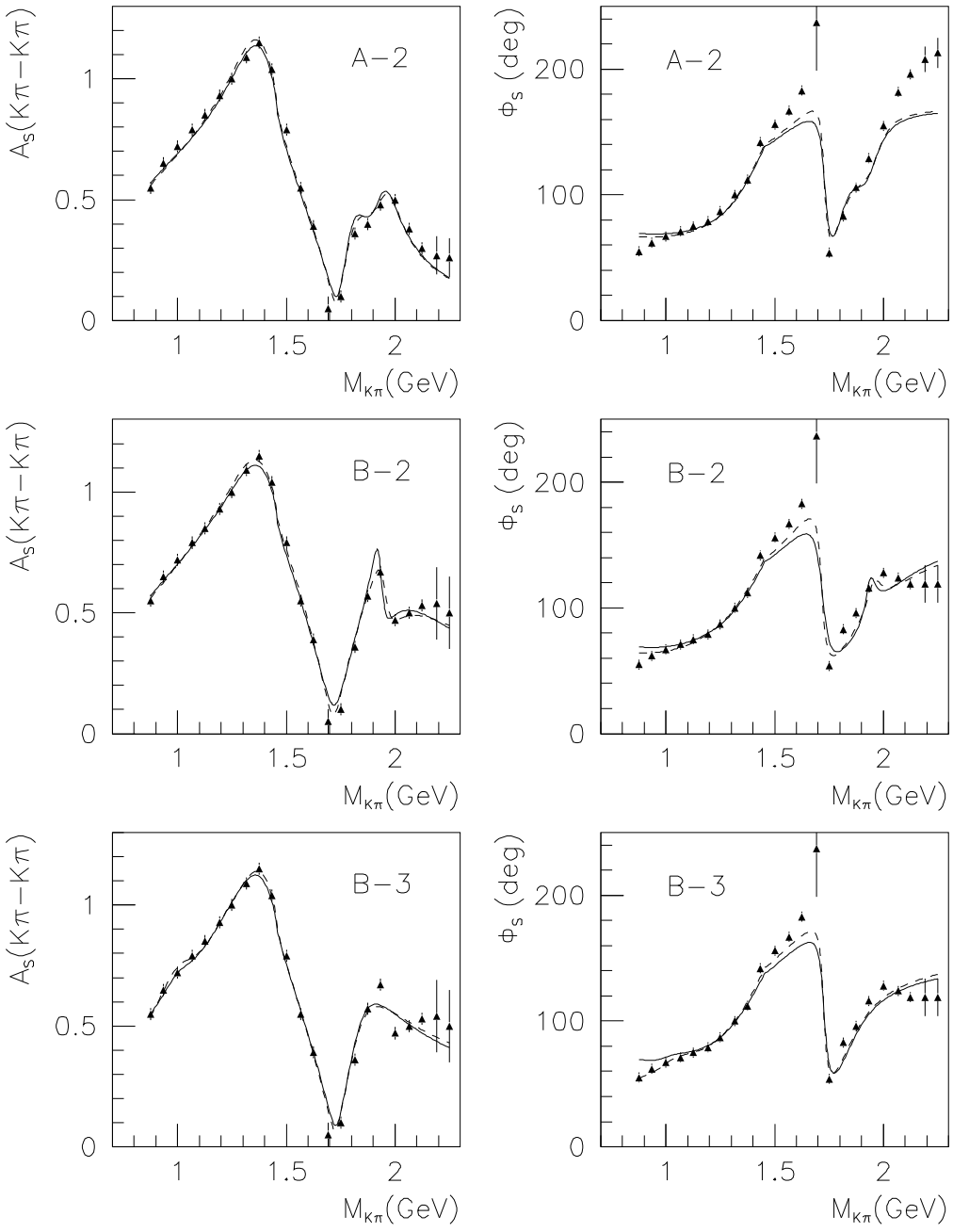

Fig. 3. The description of the data of ref. [7] by three-pole K-matrix solutions A-2, B-2 and B-3. The definition of curves is the same as in Fig. 2.

References

[1] V.V. Anisovich and A.V. Sarantsev, Phys. Lett., **B382** (1996) 429.

[2] V.V. Anisovich, Yu.D. Prokoshkin, and A.V. Sarantsev, Phys. Lett., **B389** (1996) 388.

[3] A.V. Anisovich, V.V. Anisovich and A.V.Sarantsev, "Scalar glueball: analysis of the $(IJ^{PC} = 00^{++})$-wave", hep-ph/9702339, Z.Phys.A, in press;
"0^{++}-glueball/$q\bar{q}$-state mixing in the mass region near 1500 MeV", hep-ph/9611333, Phys. Lett.B, **B395** (1997) 123.

[4] A.V. Anisovich, V.V. Anisovich, Yu.D. Prokoshkin, and A.V. Sarantsev: Z. Phys. **A357** (1997) 123.

[5] G.S. Bali et al.: Phys. Lett., **B309** (1993) 378;
J. Sexton, A. Vaccarino, and D. Weingarten: Phys. Rev. Lett., **75** (1995) 4563;
F.E. Close and M.J. Teper: "On the lightest scalar glueball", preprint RAL-96-040 (1996).

[6] V.V. Anisovich, A.A. Kondashov, Yu.D. Prokoshkin, S.A. Sadovsky and A.V. Sarantsev, Z.Phys.A, to be publish.

[7] D. Aston et al., Nucl.Phys. **B296** (1988) 493.

[8] Ch. Ritter, B.Ch. Metsch, C.R. Muenz, and H.R. Petry: Phys. Lett., **B380** (1996) 431;
F.E. Close, Yu. Dokshitzer, V.N. Gribov et al. Phys. Lett. **B319** (1993) 291.

[9] V.V. Anisovich et al.: Phys. Lett. **B323** (1994) 233;
C. Amsler et al.: Phys. Lett. **B342** (1995) 433; **B355** (1995) 425.

[10] V.V. Anisovich, D.V. Bugg, A.V. Sarantsev and B.S. Zou, Phys.Rev., **D50** (1994) 1972;
D.V. Bugg, V.V. Anisovich, A.V. Sarantsev and B.S. Zou, Phys.Rev., **D50** (1994) 4412;
D.V. Bugg, A.V. Sarantsev and B.S. Zou, Nucl.Phys., **B471** (1996) 59;
Crystal Barrel Collaboration, A.Abele et al: Nucl. Phys. **A609** (1996) 562.

[11] B. Hyams et al: Nucl. Phys. **B64** (1973) 134.

[12] D. Alde et al: Z. Phys.**C66** (1995) 375;
A.A. Kondashov et al: Proc. 27th Intern. Conf. on High Energy Physics, Glasgow (1994) 1407;
Yu.D. Prokoshkin et al: Physics-Doklady **342** (1995) 473;
A.A. Kondashov et al: Preprint IHEP 95-137, Protvino (1995);
F. Binon et al: Nuovo Cim. **A78** (1983) 313; **A80** (1984) 363.

[13] S.J. Lindenbaum and R.S. Longacre: Phys. Lett. **B274** (1992) 492;
A. Etkin et al: Phys. Rev. **D25** (1982) 1786.

[14] Particle Data Group, Phys.Rev., **D54** (1996).

[15] G. t'Hooft: Nucl. Phys., **B72** (1974) 461;
G. Veneziano: Nucl. Phys., **B117** (1976) 519.

[16] V.V. Anisovich, M.G. Huber, M.N. Kobrinsky and B.Ch. Metsch, Phys.Rev.**D42** (1990) 3045.

[17] V.V. Anisovich, Phys.Lett **B364** (1995) 195.

[18] V.V. Anisovich et al. Phys. Lett., **B355** (1995) 363;
D.V. Bugg and B.S. Zou: Phys. Rev. **D50** (1994) 591;
K.L. Au, D.Morgan and M.R. Pennington: Phys. Rev. **D35** (1987) 1633.